DOI: 10.1002/cphc.200900903

A Theoretical Study on the Mechanism of C_2H_4 Oxidation over a Neutral V_3O_8 Cluster

Yan-Ping Ma,[a, b] Xun-Lei Ding,[a] Yan-Xia Zhao,[a] and Sheng-Gui He*[a]

Density functional theory (DFT) calculations are used to investigate the reaction mechanism of $V_3O_8 + C_2H_4$. The reaction of V_3O_8 with C_2H_4 produces $V_3O_7CH_2 + HCHO$ or $V_3O_7 + CH_2OCH_2$ overall barrierlessly at room temperature, whereas formation of hydrogen-transfer products $V_3O_7 + CH_3CHO$ is subject to a tiny overall free energy barrier (0.03 eV), although the formation of the last-named pair of products is thermodynamically more favorable than that of the first two. These DFT results are in agreement with recent experimental observations. The $(O_b)_2V(O_tO_t)^\bullet$ (b = bridging, t = terminal) moiety containing the oxygen radical in V_3O_8 is the active site in the reaction with C_2H_4. Similarities and differences between the reactivities of $(O_b)_2V(O_tO_t)^\bullet$ in V_3O_8 and the small VO_3 cluster $[(O_t)_2VO_t^\bullet]$ are discussed. Moreover, the effect of the support on the reactivity of the $(O_b)_2V(O_tO_t)^\bullet$ active site is evaluated by investigating the reactivity of the cluster VX_2O_8, which is obtained by replacing the V atoms in the $(O_b)_3VO_t$ support moieties of V_3O_8 with X atoms (X = P, As, Sb, Nb, Ta, Si, and Ti). Support X atoms with different electronegativities influence the oxidative reactivity of the $(O_b)_2V(O_tO_t)^\bullet$ active site through changing the net charge of the active site. These theoretical predictions of the mechanism of $V_3O_8 + C_2H_4$ and the effect of the support on the active site may be helpful for understanding the reactivity and selectivity of reactive $O^\bullet$ species over condensed-phase catalysts.

1. Introduction

The oxidation of hydrocarbons over metal oxide catalysts, especially vanadium oxide based catalysts, is a very important catalytic process in the chemical industry.[1,2] Well-known industrial processes facilitated by vanadium oxide based catalysts include the selective oxidation of propane to acrylic acid, conversion of butane or benzene to maleic anhydride, and oxidation of naphthalene or *o*-xylene to phthalic anhydride. Chemical reactions in the above mentioned and many other catalytic processes usually occur at specific (active) sites.[3] However, the nature of the active site and features that control its reactivity and selectivity at the molecular level are usually unclear. Gas-phase clusters whose bonding and reactivity can be well interpreted by both experimental and theoretical methods are considered to be ideal model systems for local active sites of condensed-phase catalysts.[4]

To understand the mechanism of hydrocarbon oxidation on the active sites of the vanadium oxide catalytic surface, great efforts have been devoted to investigating the chemistry (structural, bonding, and reactivity properties, etc.) of vanadium oxide clusters in the gas phase by using experimental techniques based on mass spectrometry in conjunction with theoretical calculations.[5–9] However, the investigated species are mostly ionic vanadium oxide clusters. Only a few experimental studies have been carried out for neutral transition metal oxide clusters, since these clusters are difficult to detect without fragmentation. Recently, single-photon ionization through vacuum ultraviolet radiation and soft X-ray lasers has been effectively employed to detect neutral transition metal oxides without fragmentation.[10,11] The reactivity of neutral vanadium oxide clusters toward hydrocarbons such as ethane (C_2H_6), alkenes (C_2H_4, C_3H_6, C_4H_8, etc.), acetylene (C_2H_2), and benzene (C_6H_6) has been successfully studied. An interesting result is that oxygen-rich vanadium oxide clusters $VO_3(V_2O_5)_{n=0,1,2}$ exhibit particular activities with regard to C=C bond cleavage of alkenes.

On the basis of density functional theory (DFT) calculations, the reaction mechanism of neutral VO_3 cluster with C_2H_4 was investigated.[10] The calculated results indicated that the oxygen-transfer reaction channel ($VO_3 + C_2H_4 \rightarrow VO_2 + CH_3CHO$) is thermodynamically more favorable than the C=C bond-cleavage channel ($VO_3 + C_2H_4 \rightarrow VO_2CH_2 + HCHO$), but the former is kinetically less favorable than the latter at room temperature due to the overall reaction barrier (0.18 eV). The oxidative reactivity of the neutral VO_3 cluster is attributed to the existence of an unpaired electron mostly localized over one of the terminal oxygen atoms. That is, a radical oxygen center $O^\bullet$ in VO_3 leads to the oxidative reactivity of this cluster. Therefore, the reactivity of the VO_3 cluster in the gas-phase experiment is well interpreted by these theoretical findings. However, the reaction mechanisms of C_2H_4 oxidation over larger neutral clusters such as V_3O_8 have not yet been investigated. Since V_3O_8 is the smallest polynuclear neutral vanadium oxide cluster

[a] *Dr. Y.-P. Ma, Dr. X.-L. Ding, Y.-X. Zhao, Prof. Dr. S.-G. He*
State Key Laboratory for Structural Chemistry
of Unstable and Stable Species
Beijing National Laboratory for Molecular Sciences (BNLMS)
Beijing 100190 (P. R. China)
Fax: (+) 86-10-62559373
E-mail: shengguihe@iccas.ac.cn

[b] *Dr. Y.-P. Ma*
State Key Laboratory for Polymer Physics and Chemistry
Institute of Chemistry, Chinese Academy of Sciences
Beijing 100190 (P. R. China)

that was experimentally observed to cause C=C bond cleavage of C_2H_4, it is interesting to address theoretically whether the reactivity of V_3O_8 is similar to or different from that of VO_3.

Herein, the reaction mechanism of $V_3O_8 + C_2H_4$ is theoretically investigated. In the most stable structure of the neutral V_3O_8 cluster,[10,12] which has one unpaired electron, a $[(O_b)_2V(O_tO_t)^\bullet]$ moiety connects two $(O_b)_3VO_t$ units that have relatively high chemical stability. The symbols O_b and O_t represent bridging and terminal oxygen atoms, respectively. Thus, the structure of V_3O_8 can be considered as an active site $[(O_b)_2V(O_tO_t)^\bullet]$ connected to two $(O_b)_3VO_t$ supporting moieties through two O_b atoms. Comparison of the reactivity of V_3O_8 with that of VO_3 may reflect the effect of the support on the reactivity of the $O^\bullet$ center. With the motivation of gaining further information on the support effect, we also investigated the reactivity of substituted VX_2O_8 clusters, obtained by replacing the V atoms in both of the $(O_b)_3VO_t$ moieties of V_3O_8 with X atoms (X = P, As, Sb, Nb, Ta, Si, and Ti). Over condensed-phase vanadium oxide based catalysts, radical oxygen ($O^\bullet$) species were experimentally evidenced in selective oxidation of propene,[13] methane,[14] ethane,[15] and benzene.[16] The present DFT results on neutral clusters with $O^\bullet$ centers may provide molecular-level information such as chemical structures, reaction mechanisms, and support effects for the active $O^\bullet$ species over condensed-phase catalysts.

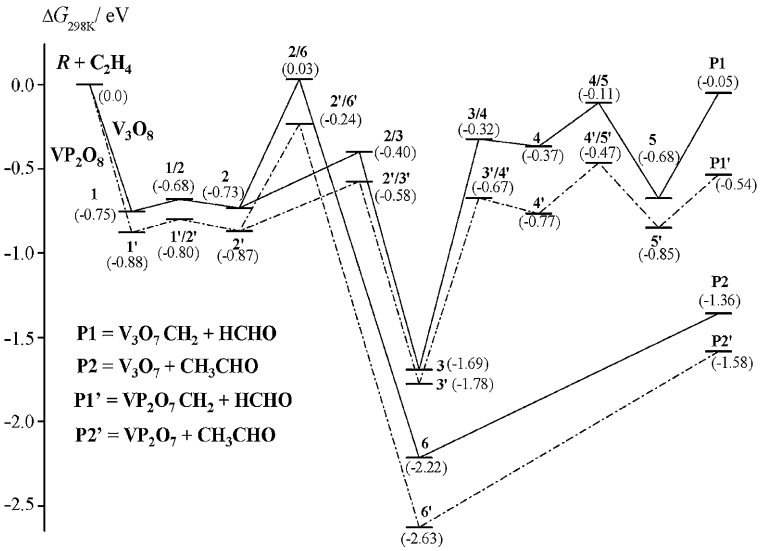

Figure 1. Potential-energy profiles for reactions of $V_3O_8 + C_2H_4$ to produce $V_3O_7CH_2 + HCHO$ (**P1**) and $V_3O_7 + CH_3CHO$ (**P2**) (——) and of $VP_2O_8 + C_2H_4$ to produce $VP_2O_7CH_2 + HCHO$ (**P1′**) and $VP_2O_7 + CH_3CHO$ (**P2′**) (–•–•). An integer ***n*** is used to denote a reaction intermediate, and two-integer combinations n_1/n_2 to denote a transition state that connects reaction intermediates n_1 and n_2. Values in parentheses are relative Gibbs free energies [eV] at 298 K with respect to the separated reactants ($R + C_2H_4$).

2. Results

2.1. Reactions of V_3O_8 with C_2H_4

The following channels were calculated for $V_3O_8 + C_2H_4$ [Eqs. (1)–(3)].

$$V_3O_8 + C_2H_4 \rightarrow V_3O_7CH_2 + HCHO \quad \Delta H_{298\,K} = -0.04\ \text{eV} \quad \text{(formaldehyde)} \tag{1}$$

$$V_3O_8 + C_2H_4 \rightarrow V_3O_7 + CH_3CHO \quad \Delta H_{298\,K} = -1.32\ \text{eV} \quad \text{(acetaldehyde)} \tag{2}$$

$$V_3O_8 + C_2H_4 \rightarrow V_3O_7 + CH_2OCH_2 \quad \Delta H_{298\,K} = -0.02\ \text{eV} \quad \text{(ethylene oxide)} \tag{3}$$

The enthalpies of reaction $\Delta H_{298\,K}$ are given for the lowest energy structures of the reactants and products in the singlet or doublet spin states. These reaction channels are all thermodynamically allowed. The Gibbs free-energy profiles for reactions (1) and (2) are plotted in Figure 1, and the structures of the reaction intermediates and transition states (TSs) in Figure 1 for $V_3O_8 + C_2H_4$ are shown in Figure 2. Formation of $V_3O_7CH_2 + HCHO$ in reaction (1) involves C=C bond cleavage, whereas formation of $V_3O_7 + CH_3CHO$ in reaction (2) involves hydrogen transfer. Figure 1 indicates that the C=C bond-cleavage process is overall barrierless at room temperature, while the hydrogen transfer process is subject to a tiny overall free-energy barrier (0.03 eV). Figure 3 plots the potential-energy profile and related structures for reaction (3). Formation of the products V_3O_7 and CH_2OCH_2 is thermodynamically and kinetically favorable at room temperature.

In the C=C bond-cleavage reaction of $V_3O_8 + C_2H_4$, intermediate **3** with a five-membered ring structure is formed through [3+2] cycloaddition. The process ($V_3O_8 + C_2H_4 \rightarrow$ **1** $\rightarrow$ **1/2** $\rightarrow$ **2** $\rightarrow$ **2/3** $\rightarrow$ **3**) to form intermediate **3** is overall barrierless, and considerable net Gibbs free energy (1.69 eV) is released. The C=C bond in the C_2H_4 moiety of **3** is greatly activated toward a single bond (1.53 Å) compared with that in the free C_2H_4 molecule (1.33 Å). The amount of free energy released is enough to overcome any barriers in the subsequent steps from **3** to the final products $V_3O_7CH_2 + HCHO$. By surmounting the **3/4** barrier, the C–C bond in **3** ruptures, yielding intermediate **4** in which two HCHO moieties are almost formed. Subsequently, via TS **4/5**, a V-O-C three-membered ring is formed in **5** from one of the HCHO moieties in **4**, and the V–O bond between the other HCHO moiety and other part of the cluster is weakened, as can be seen from the change in V–O bond length (from 1.91 in **4** to 2.11 Å in **5**). Finally, products $V_3O_7CH_2 + HCHO$ are released.

Transfer of one hydrogen atom starting from structure **2** results in formation of acetaldehyde (**2** $\rightarrow$ **2/6** $\rightarrow$ **6** $\rightarrow$ **P2**). This process is subject to an energy barrier of 0.76 eV. However, the free energy released in the formation of **2** is not sufficient to overcome this barrier. Thus, a tiny positive overall free-energy barrier (0.03 eV, Figure 1) must be surmounted for this hydrogen-transfer process. Ethylene oxide can be formed overall barrierlessly starting from intermediate **1** (**1** $\rightarrow$ **1/7** $\rightarrow$ **7** $\rightarrow V_3O_7 + CH_2OCH_2$). However, a higher binding energy (0.85 eV) be-

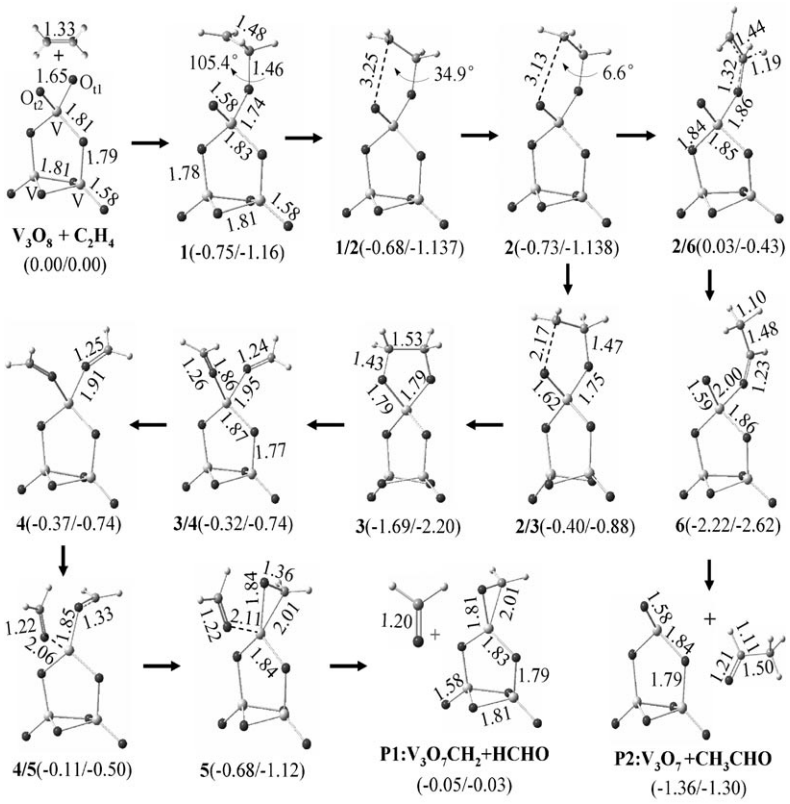

Figure 2. DFT-optimized structures of intermediates and the transition states for V_3O_8 species in Figure 1. The relative Gibbs free energies ($\Delta G_{298\,K}$ [eV]) and energies corrected for zero-point vibration ($\Delta H_{0\,K}$ [eV]) with respect to $V_3O_8 + C_2H_4$ are given in parentheses ($\Delta G_{298\,K}/\Delta H_{0\,K}$). The bond lengths are given in angstrom.

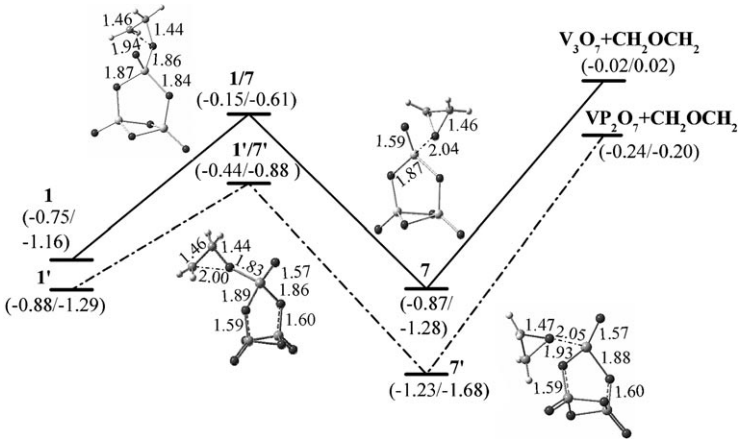

Figure 3. Potential-energy profiles for $V_3O_8 + C_2H_4 \rightarrow V_3O_7 + CH_2OCH_2$ (——) and $VP_2O_8 + C_2H_4 \rightarrow VP_2O_7 + CH_2OCH_2$ (–•–•). The DFT-optimized structures of the species in these two reactions are shown. The relative Gibbs free energies ($\Delta G_{298\,K}$ [eV]) and energies corrected for zero-point vibration ($\Delta H_{0\,K}$ [eV]) with respect to the separated reactants ($R + C_2H_4$) are given in parentheses ($\Delta G_{298\,K}/\Delta H_{0\,K}$). The bond lengths are given in angstrom.

tween ethylene oxide and V_3O_7 makes formation of separated products ($V_3O_7 + CH_2OCH_2$) thermodynamically slightly less favorable than formation of $V_3O_7CH_2 + HCHO$.

From the above reaction paths of $V_3O_8 + C_2H_4$, we can conclude that the $(O_b)_2V(O_tO_t)^{\bullet}$ moiety containing the radical oxygen center in V_3O_8 acts as the active site in the oxidation of C_2H_4, because the two support moieties $(O_b)_3VO_t$ do not participate directly in the reactions.

2.2. Reactions of VX_2O_8 with C_2H_4

The two unreactive $(O_b)_3VO_t$ units in the V_3O_8 cluster can be considered as stable support moieties connected to the active site $(O_b)_2V(O_tO_t)^{\bullet}$. By replacing the V atoms of both $(O_b)_3VO_t$ moieties in V_3O_8 with X atoms (X = P, As, Sb, Nb, Ta, Si, and Ti), we obtain the substituted clusters VX_2O_8. The support effect on the reactivity of the $(O_b)_2V(O_tO_t)^{\bullet}$ active site can be evaluated by investigating the reactivity of VX_2O_8 clusters. Figure 4 shows the optimized structures of these neutral VX_2O_8 clusters. As shown in Figure 4, the bond lengths, especially those of X–O_b bonds vary with the composition of the support moieties. For instance, the X–O_{b1} bond in VX_2O_8 clusters (X = Sb, Nb, Ta) is elongated by about 0.15 Å and the X–O_{b1} bond in VX_2O_8 (X = P, Si) shortened by more than 0.11 Å compared with the V_s–O_{b1} bond (1.793 Å) in V_3O_8 (V_s represents the V atom in the $(O_b)_3VO_t$ support moieties of V_3O_8). However, the V–O bond lengths in the $(O_b)_2V(O_tO_t)^{\bullet}$ moieties of VX_2O_8 are not changed much (within 0.02 Å) compared with those in V_3O_8. This indicates that the structure of the $(O_b)_2V(O_tO_t)^{\bullet}$ active site in each VX_2O_8 cluster is not influenced much by the different compositions of the support moieties. The singly occupied molecular orbitals (SOMOs) of VX_2O_8 clusters are shown in Figure 5, which shows that the SOMOs of these clusters have similar shapes and are generally localized on the 2p orbitals of the two O_t atoms in the $(O_b)_2V(O_tO_t)^{\bullet}$ moieties. These results suggest that the VX_2O_8 clusters could exhibit similar reactivities.

Two reaction channels are considered for $VX_2O_8 + C_2H_4$: $VX_2O_8 + C_2H_4 \rightarrow VX_2O_7CH_2 + HCHO$, $VX_2O_8 + C_2H_4 \rightarrow VX_2O_7 + CH_3CHO$. As shown in Figure 6, the reaction channels to produce HCHO (L1, −0.02 to −0.25 eV) and CH_3CHO (L2, −1.25 to −1.58 eV) are both thermodynamically allowed at room temperature. The relationship between the Gibbs free-energy changes $\Delta G_{298\,K}$ of these two channels and the total charges (denoted C_a)[17] on the $(O_b)_2V(O_tO_t)^{\bullet}$ active site is plotted in Figure 6. Good correlation be-

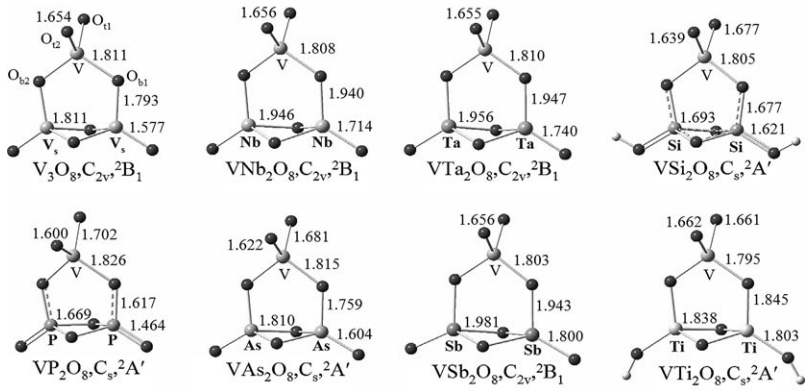

Figure 4. DFT-optimized structures of VX_2O_8 clusters (X = Ti, Si, V, P, As, Nb, Ta, and Sb) with bond lengths [Å]. The terminal oxygen atoms bonded with Ti and Si are saturated with hydrogen atoms; for convenience, the $VX_2H_2O_8$ clusters (X = Ti, Si) are denoted as VX_2O_8.

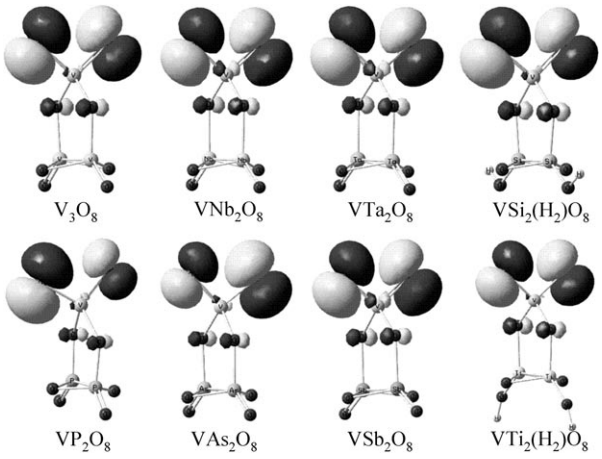

Figure 5. SOMOs of the VX_2O_8 clusters in Figure 4.

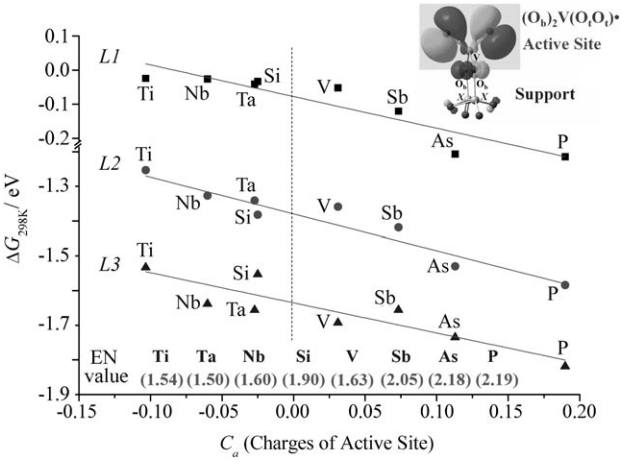

Figure 6. Plot of $\Delta G_{298\,K}$ values of three reactions versus the C_a values of the $(O_b)_2V(O_tO_t)^\bullet$ active site in VX_2O_8 clusters (X = Ti, Si, V, P, As, Nb, Ta, Sb). The three reactions are $VX_2O_8 + C_2H_4 \rightarrow VX_2O_7CH_2 + HCHO$ (L1), $VX_2O_8 + C_2H_4 \rightarrow VX_2O_7 + CH_3CHO$ (L2), and $VX_2O_8 + C_2H_4 \rightarrow VX_2O_8C_2H_4$ (L3), in which $VX_2O_8C_2H_4$ are structures with -V-O-C-C-O- rings, such as **3** or **3**′ in Figure 1. The electronegativity (EN) values of the X atoms are given in parentheses.

tween ΔG and C_a is found: ΔG tends to decrease as C_a increases. The ΔG values for the channel to produce $VX_2O_7CH_2 + HCHO$ decrease in the sequence: -0.024 eV (VTi_2O_8) > -0.026 eV (VNb_2O_8) > -0.044 eV (VTa_2O_8) > -0.052 eV (V_3O_8) > -0.120 eV (VSb_2O_8) > -0.246 eV (VAs_2O_8) > -0.254 eV (VP_2O_8), the same as the sequence of ΔG values of the channel producing $VX_2O_7 + CH_3CHO$. This sequence is found to coincide with the increasing order of the C_a values. Although the VSi_2O_8 cluster does not fit in the sequence well, the good relationship between ΔG and C_a for most of the clusters suggests that the reactivity of the $(O_b)_2V(O_tO_t)^\bullet$ active site is relevant to its charge distribution.

To gain detailed insight into the effect of the support on the reactivity of the $(O_b)_2V(O_tO_t)^\bullet$ active site, the reaction mechanisms of $VP_2O_8 + C_2H_4$ to generate $VP_2O_7CH_2 + HCHO$, $VP_2O_7 + CH_3CHO$, and $VP_2O_7 + CH_2OCH_2$ were calculated. The Gibbs free-energy profiles for HCHO and CH_3CHO formation are plotted in Figure 1, and the energy profile for CH_2OCH_2 formation in Figure 3. The structures of the reaction intermediates and TSs for $VP_2O_8 + C_2H_4$ in Figure 1 are shown in Figure 7. From Figures 1, 3, and 7 we can conclude that the reaction energy profiles and the structures of the reacting species of $VP_2O_8 + C_2H_4$ are similar to the corresponding species of $V_3O_8 + C_2H_4$. The relative Gibbs free energies of the reacting species for $VP_2O_8 + C_2H_4$ are generally lower than those for $V_3O_8 + C_2H_4$, and this reflects the higher reactivity of VP_2O_8 compared to V_3O_8. In the C=C bond-cleavage reaction channel, the free energies are lower by 0.12–0.18 eV for the process to form the cycloaddition intermediate **3**′ in $VP_2O_8 + C_2H_4$ than to form **3** in $V_3O_8 + C_2H_4$, while the energies are lower by 0.40–0.49 eV in the following steps to cleave the C=C bond and finally to evaporate the HCHO molecule. The positive overall energy barrier TS **2/6** (0.03 eV) in the hydrogen-transfer process of $V_3O_8 + C_2H_4$ to produce CH_3CHO is lowered to negative overall barrier TS **2**′/**6**′ (-0.24 eV) in $VP_2O_8 + C_2H_4$.

From the above reaction mechanisms of $V_3O_8 + C_2H_4$ and $VP_2O_8 + C_2H_4$, we can conclude that formation of the cycloaddition intermediates (similar to **3** in Figure 2) is critical in the reactions $VX_2O_8 + C_2H_4$ to produce C=C cleavage products. The relative free energies of these cycloaddition intermediates were also calculated. The good correlation found between ΔG of the cycloaddition intermediates and C_a values (L3 in Figure 6) suggests that the reaction energy profiles of other $VX_2O_8 + C_2H_4$ (X ≠ P, V) reactions may be proposed on the basis of those of $V_3O_8 + C_2H_4$ and $VP_2O_8 + C_2H_4$ by shifting the energy profile by appropriate values.

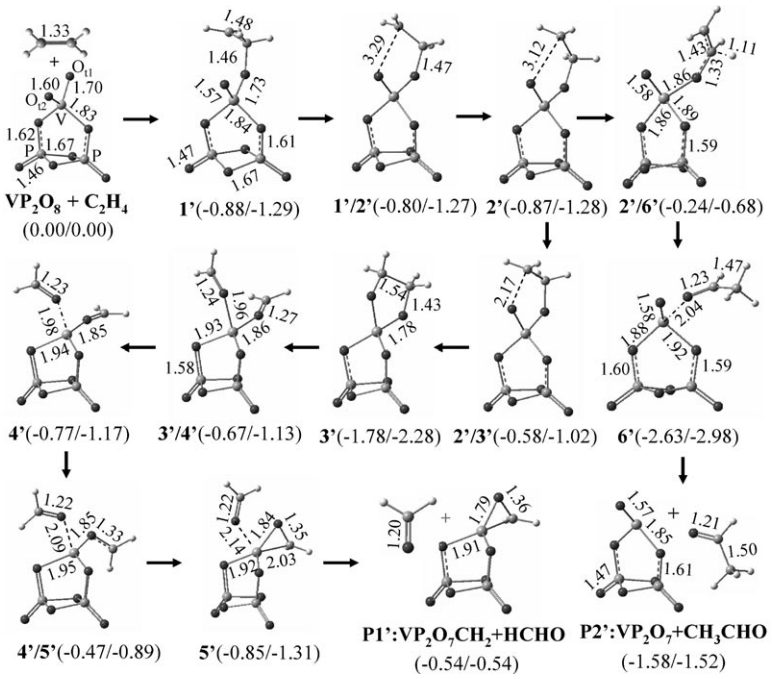

Figure 7. DFT-optimized structures of intermediates and the transition states for VP_2O_8 species in Figure 1. The relative Gibbs free energies ($\Delta G_{298\,K}$ [eV]) and energies corrected for zero-point vibration ($\Delta H_{0\,K}$ [eV]) with respect to $VP_2O_8 + C_2H_4$ are given in parentheses ($\Delta G_{298\,K}/\Delta H_{0\,K}$). The bond lengths are given in angstrom.

3. Discussion

3.1. Comparison of $V_3O_8 + C_2H_4$ with $VO_3 + C_2H_4$

In a previous work, the reactivities of neutral vanadium oxide clusters toward C_2H_4 were investigated near room temperature.[10] Product $V_3O_7CH_2$ is observed. The current DFT study (Figures 1 and 2) suggests that $V_3O_8 + C_2H_4 \rightarrow V_3O_7CH_2 + HCHO$ is the most favorable reaction channel in the reaction of V_3O_8 with C_2H_4, which is consistent with the experimental findings. The DFT calculations also suggest that V_3O_7 products can be formed from $V_3O_8 + C_2H_4$, as reaction (3) has negative overall free-energy barrier at room temperature. The $\Delta H_{0\,K}$ values listed in Figure 2 indicate that V_3O_7 can also be generated from reaction (2), provided that the reaction intermediates are not fully at thermal equilibrium due to the relatively low pressure in the fast-flow reaction experiments.[10] However, the V_3O_7 product can not be easily differentiated from the unchanged V_3O_7 in the reactivity study on the neutral cluster, since one can not mass-select neutral V_3O_8 for reactivity studies.

We previously demonstrated that the C=C bond-cleavage process also occurs barrierlessly in the reaction $VO_3 + C_2H_4$,[10] which is supported by observation of the VO_2CH_2 product experimentally. The generality of C=C bond cleavage of C_2H_4 over VO_3 and V_3O_8 clusters can be summarized as follows: the large amount of energy released in the [3+2] cycloaddition process is sufficient to break the weakened C=C bond (e.g., C–C of **3** in Figure 2) and evaporate an aldehyde fragment. The above similarity indicates that the oxidative $(O_b)_2V(O_tO_t)^{\bullet}$ moiety in V_3O_8 and the small VO_3 cluster $[(O_t)_2V(O_t)^{\bullet}]$ exhibit similar reactivity of causing C=C bond cleavage of C_2H_4. Similar to V_3O_8, the observation of the $V_5O_{12}CH_2$ product in the gas-phase experiments[10] suggests that the $(O_b)_2V(O_tO_t)^{\bullet}$ moiety could also be the active site for V_5O_{13}. A simple skeleton of the structure transformation in the general C=C bond cleavage process can be proposed as shown in Figure 8 for reactions between C_2H_4 and clusters with $(O_b)_2V(O_tO_t)^{\bullet}$ active site.

Although there is similarity between $V_3O_8 + C_2H_4$ and $VO_3 + C_2H_4$ in formaldehyde (HCHO) formation, obvious differences can be found between these two reaction systems. The major difference lies in the thermodynamics of CH_2OCH_2 formation. The DFT calculations indicate that formation of CH_2OCH_2 from $VO_3 + C_2H_4$ is endothermic ($\Delta H_{298\,K} = 0.47$ eV), while it is exothermic ($\Delta H_{298\,K} = -0.02$ eV) from $V_3O_8 + C_2H_4$. Other differences can also be found by detailed comparison of the reaction mechanisms of $VO_3 + C_2H_4$ and $V_3O_8 + C_2H_4$. In formation of the C=C bond-cleavage products $(V_2O_5)_{0,1}VO_2CH_2 + HCHO$, the Gibbs free-energy release from $VO_3 + C_2H_4$ is greater than that from $V_3O_8 + C_2H_4$ by 0.21 eV, whereas the energy release to produce oxygen-transfer products $(V_2O_5)_{0,1}VO_2 + CH_3CHO$ is smaller by 0.50 eV. The formation of CH_3CHO is subject to lower overall free-energy barrier over

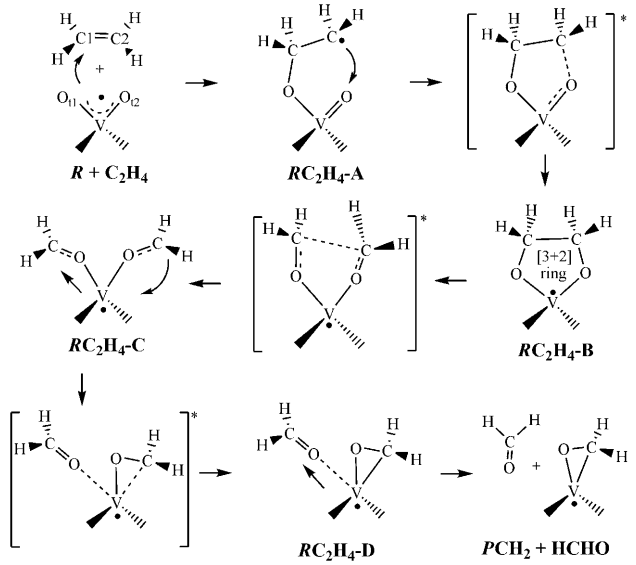

Figure 8. Simple skeleton of the structural transformation in the general C=C bond cleavage process for reactions between C_2H_4 and clusters with an $(O_b)_2V(O_tO_t)^{\bullet}$ active site.

V_3O_8 than over VO_3 (0.03 vs. 0.18 eV). Similarly, the critical step (**3**→**3/4**→**4** in Figure 1) in HCHO formation is subject to higher free-energy barrier in $V_3O_8+C_2H_4$ than in $VO_3+C_2H_4$ (1.37 versus 1.12 eV[10]). These results indicate that the V_3O_8 cluster oxidizes C_2H_4 to produce CH_3CHO or CH_2OCH_2 more favorably, while production of HCHO is less favorable in comparison with VO_3.

3.2. Support Effect

The oxidative ability of the O• center in the $(O_b)_2V(O_tO_t)$• active site changes when the V atoms in the $(O_b)_3VO_t$ support moieties in V_3O_8 are replaced by X atoms. As shown in Figure 6, good correlation between C_a and $\Delta G_{298\,K}$ (L1, L2, L3) values is found. The electronegativity (EN) values of the X atoms, listed in Figure 6, were found to be closely related to the C_a value for the corresponding VX_2O_8 cluster. For most of the VX_2O_8 clusters, the X atom with the higher EN can induce the $(O_b)_2V(O_tO_t)$• active site to have a more positive charge (higher C_a value). The reactions of $VX_2O_8+C_2H_4$ to produce $VX_2O_7+CH_3CHO$ can be considered as two steps: 1) $VX_2O_8\rightarrow VX_2O_7+O$; 2) $C_2H_4+O\rightarrow CH_3CHO$. Therefore, we can conclude that the V–O_t bond in $(O_b)_2V(O_tO_t)$• with more positive charge is relatively weak (with smaller bond energy). Thus, the support moieties influence the oxidative reactivity by changing the net charge on the $(O_b)_2V(O_tO_t)$• active site. As shown in Figure 6, the VP_2O_8 cluster is more oxidative toward C_2H_4 than V_3O_8, since the phosphorus atom (2.19) has a higher EN value than the vanadium atom (1.65).

The similar structures of reaction species and energy profiles for reactions $VP_2O_8+C_2H_4$ and $V_3O_8+C_2H_4$ can be interpreted by the similar structure of the $(O_b)_2V(O_tO_t)$• active site and the similar distributions of the SOMOs of VP_2O_8 and V_3O_8. Consequently, the structures of reaction species and free-energy profiles for other reactions $VX_2O_8+C_2H_4$ (X≠P, V) can be proposed. The simple skeleton of the structural transformation for the C=C bond cleavage process in Figure 8 can also be applied to the reactions $VX_2O_8+C_2H_4$ (X≠P, V) producing $VX_2O_7CH_2+HCHO$. The relative free energies of each intermediate or TS for these reactions may be deduced from the relationships in Figure 6.

The charge-relevant reactivity of the $(O_b)_2V(O_tO_t)$• active site can also be understood by comparison of the reactivities of $V_2O_5^+$, V_3O_8, and $V_2O_6^-$ clusters. Reactions of $V_2O_5^+$ with C_2H_4 have been investigated by DFT calculations.[5d] Formation of CH_3CHO is highly favorable and supports the experimental observations of $V_2O_4^+$ as main reaction product. Besides, similar to $V_3O_8+C_2H_4$, a [3+2] cycloaddition species $V_2O_5C_2H_4^+$ is predicted to be lower in energy than the separated reactants by 4.44 eV, which is much larger than that for $V_3O_8C_2H_4$ (1.69 eV, species **3** in Figures 1 and 2). The large amount of energy released should be able to cleave the C=C bond and evaporate HCHO fragment(s). A side reaction channel $V_2O_5^+ + C_2H_4\rightarrow V_2O_3^+ + 2HCHO$, the calculated energy change ΔE of which is −0.65 eV, was suggested to explain the observation of $V_2O_3^+$ as minor product in the experiments.[5d,f] The stable structure of $V_2O_5^+$ proposed in the literature[5d] can be considered as a $(O_b)_2V(O_tO_t)$• moiety connected to a $(O_b)_2V(O_t)^+$ unit in which the vanadium atom is in +5 valence state, and $(O_b)_2V(O_t)^+$ as a positively charged stable support. The total charge of the $(O_b)_2V(O_tO_t)$• moiety in $V_2O_5^+$ is about +0.37, which is greater than that of the same moiety in V_3O_8 (+0.03), that is, an O_t atom is relatively weakly bonded in the $(O_b)_2V(O_tO_t)$• moiety of $V_2O_5^+$. Note that the dissociation energy of $V_2O_5^+$ ($V_2O_4^+$–O) and V_3O_8 (V_3O_7–O) are calculated to be 2.78 and 3.35 eV, respectively, at B3LYP/TZVP level of theory. These results favor formation of oxygen-transfer product CH_3CHO in $V_2O_5^+ + C_2H_4$, in agreement with the experimental observations. The $V_2O_6^-$ cluster also has a $(O_b)_2V(O_tO_t)$• moiety, and the structure of $V_2O_6^-$ can be considered as a $(O_b)_2V(O_tO_t)$• moiety connected to the negatively charged stable support $(O_b)_2V(O_tO_t)^-$.[18,19] Influenced by the anionic property of the support, the active site has net negative charge, which results in the low reactivity of the $V_2O_6^-$ cluster towards C_2H_4 oxidation.[5b] Similar to V_3O_8, if the vanadium atom in the $(O_b)_2V(O_tO_t)^-$ support moiety of $V_2O_6^-$ is replaced by atom with higher EN value, it may be possible to detect some oxidative products in the reactions with unsaturated hydrocarbons. It will be interesting to investigate the reactivity of metal- or nonmetal-doped vanadium oxide clusters in future gas-phase experiments.

3.3. Consideration of Condensed-Phase Reactions

In hydrocarbon oxidation reactions over condensed-phase catalysts, vanadium oxide based catalysts are of particular significance. Due to the complexity, a single vanadium cluster can not model all the reaction mechanisms at the molecular level for condensed-phase catalysis. However, various reaction channels in this study may provide possible reaction processes for related alkenes oxidation over various vanadium oxide catalysts.

As indicated in this study, various useful products (formaldehyde, acetaldehyde, and ethylene oxide) can be generated with negative or small positive overall barriers in the reaction of V_3O_8 with ethylene. Epoxides, especially ethylene and propene oxides, are important materials and intermediates in the chemical industry. They were detected as the major selective products in some photooxidation reactions over supported transition metal oxide catalysts including vanadium oxide.[13,20–22] The active oxygen species were suggested to be electrophilic lattice oxygen $O^{\bullet-}$ in the mechanism of photooxidation reactions over V_2O_5/SiO_2 catalysts.[22] Moreover, in the selective oxidation of propylene over vanadium oxide catalysts, the C=C bond-cleavage products acetaldehyde and CO_2 were observed to be the major products with catalysis by V_2O_5/SiO_2. Electrophilic surface oxygen species $O_2^{\bullet-}$ or $O^{\bullet-}$ were suggested to be critical to C=C bond breaking. The mechanisms of the O• species oxidizing ethylene to ethylene oxide and to the C–C bond cleavage products may be similar to those in the reaction of V_3O_8 with ethylene.

In most cases, other elements such as P, Mo, Ti, Sb are usually added as support components or promoters to vanadium oxide catalysts to improve or alter the redox abilities. The reactivity of the O• radical center was found in this work to be re-

lated to the charge properties of the O• radical center, which can be influenced by altering the support composition. Since the O• radical species are unstable, the active radical clusters may serve as surface defects and intermediate reactive centers during condensed-phase catalysis. The effect of the support on the reactivity and selectivity of reactive oxygen species over related catalysts may be understood from this study.

4. Conclusions

Density functional calculations on the reaction mechanisms of $V_3O_8 + C_2H_4$ revealed some interesting results. The reaction $V_3O_8 + C_2H_4$ produces $V_3O_7CH_2 + HCHO$ and $V_3O_7 + CH_2OCH_2$ overall barrierlessly under room-temperature conditions, whereas formation of hydrogen-transfer products $V_3O_7 + CH_3CHO$ is subject to a tiny overall free-energy barrier (0.03 eV), although the formation of the latter products is thermodynamically more favorable than that of the former two. These theoretical findings are supported by the observation of $V_3O_7CH_2$ and possibly V_3O_7 as products in the gas-phase experiments. The $(O_b)_2V(O_tO_t)^•$ moiety in V_3O_8 is the active site in its reaction towards C_2H_4 oxidation.

Similar reactivity of the $(O_b)_2V(O_tO_t)^•$ sites in V_3O_8 and the small VO_3 cluster $[(O_t)_2VO_t^•]$ was revealed in the ability to cause C=C bond cleavage of C_2H_4. However, there are obvious differences between the $V_3O_8 + C_2H_4$ and $VO_3 + C_2H_4$ systems. Formation of CH_2OCH_2 from $V_3O_8 + C_2H_4$ is much more favorable than from $VO_3 + C_2H_4$. Similarly, formation of CH_3CHO from the former is also more favorable than from the latter.

The effect of the support on the reactivity of the $(O_b)_2V(O_tO_t)^•$ active site was studied by investigating the reactivity of VX_2O_8 clusters, obtained by replacing the V atoms in the $(O_b)_3VO_t$ support moieties of V_3O_8 with X atoms, where X represents P, As, Sb, Nb, Ta, Si, and Ti. The similar structures of the $(O_b)_2V(O_tO_t)^•$ active site and the distributions of the SOMOs indicate similar reactivities of these VX_2O_8 clusters. However, the detailed oxidative ability of the $(O_b)_2V(O_tO_t)^•$ active site depends on the X atom in the support moieties. In comparison with V_3O_8, higher oxidative reactivity can be found in VX_2O_8 when X = P, As, or Sb, which has higher electronegativity than V, while VX_2O_8 exhibits lower reactivity when X = Ti, Nb, or Ta, which has lower electronegativity than V. The support moieties influence the oxidative reactivity of the $(O_b)_2V(O_tO_t)^•$ active site by changing its net charge. The $(O_b)_2V(O_tO_t)^•$ moiety with more positive charge has higher reactivity for oxidizing C_2H_4. The support effect on the reactivity and selectivity of reactive oxygen species over condensed-phase catalysts may be understood from this study.

Computational Methods

Density functional calculations using the Gaussian 03 program suite[23] were employed to study the reaction of V_3O_8 with C_2H_4. The reaction pathway calculations involve geometry optimization of various reaction intermediates and TSs. The TSs were optimized by using either the Berny algorithm[24] or the synchronous transit-guided quasi-Newton (STQN) method.[25] For most cases, initial guess structures of the TSs were obtained through relaxed potential-energy surface (PES) scans using an appropriate internal coordinate. For a few complicated cases, the initial structures were obtained by using the multicoordinate driven method,[26] which determines the relaxed PES in terms of more than one active internal coordinate. Vibrational frequencies were calculated to check that the reaction intermediates and the TSs have all positive and only one imaginary frequency, respectively. Intrinsic reaction coordinate (IRC) calculations[27] were also performed to check a TS connects two appropriate local minima in the reaction paths. Only reaction potential-energy surfaces for species in doublet states are considered, as quartet states are considerably higher in energy for reactants, products, and most of the reaction intermediates and transition states.

The Gibbs free-energy changes of $VX_2O_8 + C_2H_4$ (X = P, As, Sb, Nb, Ta, Si, and Ti) reactions were also calculated in this work. The detailed reaction mechanism of $VP_2O_8 + C_2H_4$ was also calculated. The hybrid B3LYP exchange-correlation functional[28] with the all-electron polarized triple-ζ valence basis set (TZVP)[29] has been shown previously to predict reasonably good energetics for vanadium oxide clusters and hydrocarbons at moderate computational cost.[5d,e,7a,b,30] The B3LYP functional was used throughout this work. The TZVP basis set was adopted for V, O, P, As, Si, Ti, C, and H atoms, and effective core potentials (ECPs)[31] combined with polarized triple-ζ valence basis sets (Def2-TZVP)[31,32] were used for Nb, Ta, and Sb atoms. Unless otherwise specified, the reported energies in this work are Gibbs free energies at 298 K (ΔG_{298}). Cartesian coordinates, electronic energies, and vibrational frequencies for all of the optimized structures are available upon request.

Acknowledgements

This work was supported by the Chinese Academy of Sciences (Hundred Talents Fund), the National Natural Science Foundation of China (Nos. 20703048, 20803083, and 20933008), CMS Foundation of the ICCAS (No. CMS-CX200902), and the 973 Program (No. 2006CB932100).

Keywords: cluster compounds · density functional calculations · oxidation · reaction mechanisms · vanadium

[1] a) G. Ertl, H. Knözinger, J. Weikamp, *Handbook of Heterogeneous Catalysis* Wiley-VCH: New York, **1997**; b) J. L. G. Fierro, *Metal Oxides Chemistry and Applications* Taylor & Francis Group, London, **2006**; c) B. M. Weckhuysen, D. E. Keller, *Catal. Today* **2003**, *78*, 25–46.

[2] G. Centi, F. Trifirò, J. R. Ebner, V. M. Fianchetti, *Chem. Rev.* **1988**, *88*, 55–80.

[3] a) T. Zambelli, J. Wintterlin, J. Trost, G. Ertl, *Science* **1996**, *273*, 1688–1690; b) A. T. Bell, *Science* **2003**, *299*, 1688–1691; c) J. M. Thomas, *Top. Catal.* **2006**, *38*, 3–5.

[4] a) B. de Bruin, P. H. M. Budzelaar, A. W. Gal, *Angew. Chem.* **2004**, *116*, 4236–4251; *Angew. Chem. Int. Ed.* **2004**, *43*, 4142–4157; b) D. K. Böhme, H. Schwarz, *Angew. Chem.* **2005**, *117*, 2388–2406; *Angew. Chem. Int. Ed.* **2005**, *44*, 2336–2354; c) K. A. Zemski, D. R. Justes, A. W. Castleman, Jr., *J. Phys. Chem. B* **2002**, *106*, 6136–6148; d) T. Waters, G. N. Khairallah, S. A. S. Y. Wimala, Y. C. Ang, R. A. J. O'Hair, A. G. Wedd, *Chem. Commun.* **2006**, 4503–4505; e) W. Xue, Z. C. Wang, S. G. He, Y. Xie, E. R. Bernstein, *J. Am. Chem. Soc.* **2008**, *130*, 15879–15888.

[5] a) R. C. Bell, K. A. Zemski, D. R. Justes, A. W. Castleman, Jr., *J. Chem. Phys.* **2001**, *114*, 798–811; b) K. A. Zemski, D. R. Justes, A. W. Castleman, Jr., *J. Phys. Chem. A* **2001**, *105*, 10237–10245; c) R. C. Bell, A. W. Castleman, Jr., *J. Phys. Chem. A* **2002**, *106*, 9893–9899; d) D. R. Justes, R. Mitrić, N. A. Moore, V. Bonačić-Koutecký, A. W. Castleman, Jr., *J. Am. Chem. Soc.*

2003, *125*, 6289 – 6299; e) N. A. Moore, R. Mitrić, D. R. Justes, V. Bonačić-Koutecký, A. W. Castleman, Jr., *J. Phys. Chem. B* **2006**, *110*, 3015 – 3022; f) D. R. Justes, A. W. Castleman, Jr., R. Mitrić, V. Bonačić-Koutecký, *Eur. Phys. J. D* **2003**, *24*, 331 – 334.

[6] a) M. Foltin, G. J. Stueber, E. R. Bernstein, *J. Chem. Phys.* **1999**, *111*, 9577 – 9586; b) Y. Matsuda, E. R. Bernstein, *J. Phys. Chem. A* **2005**, *109*, 3803 – 3811; c) S. G. He, Y. Xie, F. Dong, S. Heinbuch, E. Jakubikova, J. J. Rocca, E. R. Bernstein, *J. Phys.Chem. A* **2008**, *112*, 11067 – 11077.

[7] a) S. Feyel, D. Schröder, X. Rozanska, J. Sauer, H. Schwarz, *Angew. Chem.* **2006**, *118*, 4793 – 4797; *Angew. Chem. Int. Ed.* **2006**, *45*, 4677 – 4681; b) S. Feyel, J. Döbler, D. Schröder, J. Sauer, H. Schwarz, *Angew. Chem.* **2006**, *118*, 4797 – 4801; *Angew. Chem. Int. Ed.* **2006**, *45*, 4681 – 4685; c) S. Feyel, H. Schwarz, D. Schröder, C. Daniel, H. Hartl, J. Döbler, J. Sauer, G. Santambrogio, L. Wöste, K. R. Asmis, *ChemPhysChem* **2007**, *8*, 1640 – 1647; d) S. Feyel, D. Schröder, H. Schwarz, *Eur. J. Inorg. Chem.* **2008**, 4961 – 4967; e) S. Feyel, D. Schröder, H. Schwarz, *J. Phys. Chem. A* **2006**, *110*, 2647 – 2654.

[8] T. Waters, A. G. Wedd, R. A. J. O'Hair, *Chem. Eur. J.* **2007**, *13*, 8818 – 8829.

[9] W. G. Wang, Z. C. Wang, S. Yin, S. G. He, M. F. Ge, *Chin. J. Chem. Phys.* **2007**, *20*, 412 – 418.

[10] F. Dong, S. Heinbuch, Y. Xie, J. J. Rocca, E. R. Bernstein, Z. C. Wang, K. Deng, S. G. He, *J. Am. Chem. Soc.* **2008**, *130*, 1932 – 1943.

[11] F. Dong, S. Heinbuch, Y. Xie, E. R. Bernstein, J. J. Rocca, Z. C. Wang, X. L. Ding, S. G. He, *J. Am. Chem. Soc.* **2009**, *131*, 1057 – 1066.

[12] E. Jakubikova, A. K. Rappé, E. R. Bernstein, *J. Phys. Chem. A.* **2007**, *111*, 12938 – 12943.

[13] F. Amano, T. Tanaka, *Catal. Commun.* **2005**, *6*, 269 – 273.

[14] H. F. Liu, R. S. Liu, K. Y. Liew, R. E. Johnson, J. H. Lunsford, *J. Am. Chem. Soc.* **1984**, *106*, 4117 – 4121.

[15] T. J. Yang, J. H. Lunsford, *J. Catal.* **1980**, *63*, 505 – 509.

[16] a) M. Iwamoto, I. Hirata, K. Matsukami, S. Kagawa, *J. Phys. Chem.* **1983**, *87*, 903 – 905; b) G. I. Panov, K. A. Dubkov, E. V. Starokon, *Catal. Today* **2006**, *117*, 148 – 155.

[17] The C_a value is obtained from the sum of the Mulliken atomic charges of the V_1, O_{t1}, O_{t2}, and O_{b1} atoms (Figure 4). Because the clusters in Figure 4 have C_s or C_{2v} symmetry, O_{b1} and O_{b2} have the same charge distribution. Each of the O_{b1} and O_{b2} are connected with two moieties ($(O_b)_2V(O_tO_t)^{\bullet}$ and $(O_b)_3VO_t$), so their contribution to the net charge of $(O_b)_2V(O_tO_t)^{\bullet}$ can be accounted for by the net charge of a single O_{b1} or O_{b2} atom.

[18] K. R. Asmis, J. Sauer, *Mass Spectrom. Rev.* **2007**, *26*, 542 – 562.

[19] G. Santambrogio, M. Brümmer, L. Wöste, J. Döbler, M. Sierka, J. Sauer, G. Meijer, K. R. Asmis, *Phys. Chem. Chem. Phys.* **2008**, *10*, 3992 – 4005.

[20] R. M. Lambert, F. J. Williams, R. L. Cropley, A. Palermo, *J. Mol. Catal. A Chem.* **2005**, *228*, 27 – 33.

[21] F. Amano, T. Tanaka, T. Funabiki, *Langmuir* **2004**, *20*, 4236 – 4240.

[22] F. Amano, T. Yamaguchi, T. Tanaka, *J. Phy. Chem. B* **2006**, *110*, 281 – 288.

[23] *Gaussian 03, Revision C.02*, M. J. Frisch, G. W. Trucks, H. B. Schlegel, G. E. Scuseria, M. A. Robb, J. R. Cheeseman, J. A. Montgomery, Jr., T. Vreven, K. N. Kudin, J. C. Burant, J. M. Millam, S. S. Iyengar, J. Tomasi, V. Barone, B. Mennucci, M. Cossi, G. Scalmani, N. Rega, G. A. Petersson, H. Nakatsuji, M. Hada, M. Ehara, K. Toyota, R. Fukuda, J. Hasegawa, M. Ishida, T. Nakajima, Y. Honda, O. Kitao, H. Nakai, M. Klene, X. Li, J. E. Knox, H. P. Hratchian, J. B. Cross, V. Bakken, C. Adamo, J. Jaramillo, R. Gomperts, R. E. Stratmann, O. Yazyev, A. J. Austin, R. Cammi, C. Pomelli, J. W. Ochterski, P. Y. Ayala, K. Morokuma, G. A. Voth, P. Salvador, J. J. Dannenberg, V. G. Zakrzewski, S. Dapprich, A. D. Daniels, M. C. Strain, O. Farkas, D. K. Malick, A. D. Rabuck, K. Raghavachari, J. B. Foresman, J. V. Ortiz, Q. Cui, A. G. Baboul, S. Clifford, J. Cioslowski, B. B. Stefanov, G. Liu, A. Liashenko, P. Piskorz, I. Komaromi, R. L. Martin, D. J. Fox, T. Keith, M. A. Al-Laham, C. Y. Peng, A. Nanayakkara, M. Challacombe, P. M. W. Gill, B. Johnson, W. Chen, M. W. Wong, C. Gonzalez, J. A. Pople, Gaussian, Inc., Wallingford, CT, **2004**.

[24] H. B. Schlegel, *J. Comput. Chem.* **1982**, *3*, 214 – 218.

[25] a) C. Peng, H. B. Schlegel, *Isr. J. Chem.* **1993**, *33*, 449 – 454; b) C. Peng, P. Y. Ayala, H. B. Schlegel, M. J. Frisch, *J. Comput. Chem.* **1996**, *17*, 49 – 56.

[26] I. Berente, G. Naray-Szabo, *J. Phys. Chem. A* **2006**, *110*, 772 – 778.

[27] a) C. Gonzalez, H. B. Schlegel, *J. Chem. Phys.* **1989**, *90*, 2154 – 2161; b) C. Gonzalez, H. B. Schlegel, *J. Phys. Chem.* **1990**, *94*, 5523 – 5527.

[28] a) A. D. Becke, *Phys. Rev. A* **1988**, *38*, 3098 – 3100; b) A. D. Becke, *J. Chem. Phys.* **1993**, *98*, 5648 – 5652; c) C. Lee, W. Yang, R. G. Parr, *Phys. Rev. B* **1988**, *37*, 785 – 789.

[29] A. Schäfer, C. Huber, R. Ahlrichs, *J. Chem. Phys.* **1994**, *100*, 5829 – 5835.

[30] Y. P. Ma, W. Xue, Z. C. Wang, M. F. Ge, S. G. He, *J. Phys. Chem. A* **2008**, *112*, 3731 – 3741.

[31] D. Andrae, U. Häußermann, M. Dolg, H. Stoll, H. Preuß, *Theor. Chim. Acta.* **1990**, *77*, 123 – 141.

[32] F. Weigend, R. Ahlrichs, *Phys. Chem. Chem. Phys.* **2005**, *7*, 3297 – 3305.

Received: November 19, 2009
Published online on ■■ ■■, 2010

ARTICLES

The barrierless reaction of C_2H_4 with V_3O_8 at room temperature generates HCHO ($+V_3O_7CH_2$) and CH_2OCH_2 ($+V_3O_7$) according to DFT calculations. The V_3O_8 cluster can be regarded as consisting of two unreactive $(O_b)_3VO_t$ support units and an $(O_b)_2V(O_tO_t)^{\bullet}$ active site (see picture; b = bridging, t = terminal), the reactivity of which can be altered by replacing the V atoms in the support moieties with X atoms.

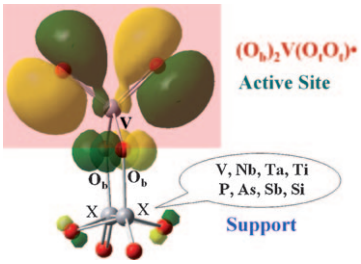

*Y.-P. Ma, X.-L. Ding, Y.-X. Zhao, S.-G. He**

■■ – ■■

A Theoretical Study on the Mechanism of C_2H_4 Oxidation over a Neutral V_3O_8 Cluster

